Available online at www.sciencedirect.com
SCIENCE DIRECT®
Journal of Molecular Catalysis B: Enzymatic 31 (2004) 123–128
JOURNAL OF MOLECULAR CATALYSIS B: ENZYMATIC
www.elsevier.com/locate/molcatb

Aldol additions with mutant lipase: analysis by experiments and theoretical calculations

Cecilia Branneby[a,1], Peter Carlqvist[b,1], Karl Hult[a], Tore Brinck[b,**], Per Berglund[a,*]

[a] *Department of Biotechnology, AlbaNova University Center, Royal Institute of Technology (KTH), SE-106 91 Stockholm, Sweden*
[b] *Department of Chemistry, Physical Chemistry, Royal Institute of Technology (KTH), SE-100 44 Stockholm, Sweden*

Received 24 June 2004; received in revised form 25 August 2004; accepted 26 August 2004
Available online 1 October 2004

Abstract

A Ser105Ala mutant of *Candida antarctica* lipase B has previously been shown to catalyze aldol additions. Quantum chemical calculations predicted a reaction rate similar to that of natural enzymes, whereas experiments showed a much lower reaction rate. Molecular dynamics simulations, presented here, show that the low reaction rate is a consequence of the low frequencies of near attack complexes in the enzyme. Equilibrium was also considered as a reason for the slow product formation, but could be excluded by performing a sequential reaction to push the reaction towards product formation. In this paper, further experimental results are also presented, highlighting the importance of the entire active site for catalysis.

Keywords: Oxyanion hole; Reaction specificity; Ab initio calculations; Lipase; Aldolase

1. Introduction

Protein engineering has been an important tool for biochemists for many years. Protein properties can be changed and new functionalities can be introduced, such as catalytic activity for new reactions. In addition to this, modeling studies and quantum mechanical (QM) calculations can be used to find the proper position for a mutation and to predict the catalytic properties of the mutant.

Candida antarctica lipase B (CALB) is a serine hydrolase that belongs to the group of α/β-hydrolases [1]. This lipase has an active site where the reaction is catalyzed by a catalytic triad (Ser105, Asp187 and His224) and an oxyanion hole (Thr40 and Gln106), which stabilizes the oxyanion intermediate [2].

A site-directed mutation to replace the active-site serine with an alanine gave an enzyme, CALB Ser105Ala, with increased activity for aldol reactions (Scheme 1) [3]. As the nucleophilic serine was removed, the basic nitrogen on the histidine was thought to get an increased ability to abstract the substrate's α-proton. An enolate intermediate is then formed, which is stabilized by hydrogen-bond donors in the oxyanion hole [3]. The experimental studies were preceded by quantum chemical calculations, which predicted that the aldol reaction would take place with a reaction rate similar to that of natural enzymes. The reaction was confirmed to take place in the active site, however, the catalytic constant was found to be only 65 day^{-1}. The reactions were run in cyclohexane, which was chosen after screening various solvents for the aldol reaction of hexanal [3]. In this article, we present molecular dynamics simulations which provide an explanation for these low reaction rates.

* Corresponding author. Tel.: +46 8 5537 8366; fax: +46 8 5537 8468.
** Co-corresponding author. Fax: +46 8 790 8207.
E-mail addresses: tore@physchem.kth.se (T. Brinck), per.berglund@biotech.kth.se (P. Berglund).
[1] Shared first authorship.

1381-1177/$ – see front matter © 2004 Elsevier B.V. All rights reserved.
doi:10.1016/j.molcatb.2004.08.005

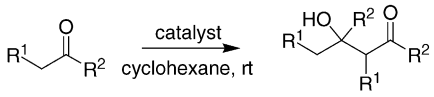

Scheme 1. The aldol reactions explored with *C. antarctica* lipase B. R^1 and R^2 are specified in Table 1.

2. Experimental

2.1. Enzyme production

C. antarctica lipase B, wild type and Ser105Ala, were produced and purified as previously described [3,4]. The purified enzymes were then immobilized at 3% (w/w) on polypropylene Accurel MP1000, <1500 μm, in 50 mM potassium phosphate buffer of pH 7.6 or 8.6, during 24 h at room temperature and end-over-end rotation. The carrier was filtered off and equilibrated over a saturated aqueous solution of NaCl to obtain a water activity of 0.75 [5].

2.2. Aldol reaction

A typical reaction mixture contained 0.3 M substrate (aldehyde/ketone), 0.003 M internal standard (hexadecane) and 66.7 mg immobilized enzyme/ml (or 1 mg imidazole/ml), in water-saturated cyclohexane. The reaction was placed in an end-over-end rotator at 20 °C. Samples were taken for analysis on GC (HP 5890 and 6890), with FID and MS detectors for quantitative and qualitative analysis, respectively. The columns used were capillary columns (J&W Cyclosil-B, 30 m × 0.32 mm i.d., d_f 0.25 μm and Wcot fused silica CP-Chirasil Dex CB 25 m × 0.32 mm i.d, d_f 0.25 μm). Helium was used both as carrier gas and make up gas.

2.3. Sequential reaction

The reaction mixture consisted of 0.30 M propanal and 0.27 M ethanethiol and 66.7 mg immobilized enzyme/ml, in water-saturated cyclohexane. The enzyme used in this experiment was immobilized at pH 8.6.

2.4. Product identification

Commercially available products were purchased and used as reference compounds (2-isopropyl-5-methyl-2-hexenal and 4-methyl-3-penten-2-one). Some products could be identified by comparing the MS fragmentation from the NIST library [6]. Those products that could not be identified by either NIST library or reference products were synthesized (2-butyl-3-hydroxy-octanal, 2-butyl-2-octenal, 3-hydroxy-5-methyl-2-(1-methylethyl)-hexanal and 5-methyl-2-(1-methylethyl)-2-hexenal), from the corresponding aldehyde (1.6 mM) in water, adjusted to pH 12, using NaOH. The reaction mixture was kept on ice, and then stopped by neutralization with HCl.

2.5. Substrate sources

All substrates and solvents were commercially available and were used without further purification.

2.6. Computational methods

The Autodock 3.0 program package was used for the docking of substrates to the mutant enzyme [7]. This program uses a Lamarckian genetic algorithm (LGA) for the automated docking of ligands to proteins. During the simulation, the interaction energy between ligand and the protein is evaluated using grid-based atomic affinity potentials. The final free energy of interaction is calculated with a free energy based expression that includes terms for the dispersion and repulsion energies, directional hydrogen bonding, screened electrostatics and desolvation. The protein structure used for the docking studies was CALB containing an *N*-hexyl phosphonate ethyl ester inhibitor (1TCA.pdb) [2]. To simulate the mutation of CALB, the Ser105 was replaced by an alanine using the SwissPDBviewer program [8] and charges for the protein atoms were taken from the original Amber united atom force field [9], as recommended in the Autodock manual. Atomic solvation parameters and fragmental volumes were assigned to the protein atoms with the program Addsol, included in the Autodock 3.0 package. The Nε2 atom of His224 was kept deprotonated in all docking simulations and for docking of the second molecule of hexanal, the first docked hexanal was treated as part of the protein. The substrate molecules were also treated using the united atom approach with charges fitted to reproduce the ab initio HF/6-31G* electrostatic potential using the procedure of Besler et al. [10]. In all the docking simulations, we used grid maps with 60 × 60 × 60 points and a spacing of 0.375 Å. The maps were centered on the Nε2 nitrogen of His224 located in the active site of CALB. A total of 50 runs using the LGA were performed in each separate case where the substrates to be docked were free to rotate around their carbon–carbon single bonds during the simulations.

Selected docked structures were used for molecular dynamics (MD) simulations to evaluate the existence and dynamics of near attack complexes (NACs) [11–13]. The program package Q was used for all MD simulations [14] and the force field employed was the Q-implementation of Amber95 [15]. Parameters for the substrates were assigned in analogy with the amino acid residue parameters of the force field. The simulations were performed on spheres with the radius of 16 Å centered on the active-site histidine (Nε2, His224). A large number of SPC waters were added to fill the simulation sphere. Protein atoms outside the sphere were held fixed during the simulations. An analysis of the hydrogen bonding pattern in the crystal structure indicated that Asp134 and Glu188 should be protonated. In the simulation

sphere only Asp187 was charged, whereas all amino acids outside the simulation sphere were treated as neutral.

The following protocol was used for the MD simulations: five warm-up steps were performed, each 4 ps long with a time step of 1 fs. The first run was performed at 1 K with a bath-coupling constant of 1, the low coupling constant makes this run much like an energy minimization. The four remaining warm-up runs used a bath-coupling constant of 5 and were performed at 50, 150 K, and the last two at 300 K, respectively. In the first four warm-up simulations, all protein and substrate atoms are restrained to their initial coordinates by a 5 kcal/(mol Å^2) harmonic potential. In the final warm-up run, all atoms in the simulation sphere were free to move. For the actual MD simulations, 20 runs, each 50 ps long were performed, giving a total simulation time of 1 ns. The simulation temperature was 300 K, with a bath-coupling constant of 10 and a time step of 1 fs. For the analysis of the MD simulations, the visualization program VMD [16] was used. When considering what would account for NACs for the proton transfer step and the addition step, the sum of the van der Waals radii were used to define a minimum reaction distance. For a more quantitative analysis, a more detailed description of NAC should be used. However, this simplified model was found to be sufficient to give a qualitative explanation for the low reaction rate observed in experiments. For reference, it should be noted that the frequency of NAC formation in natural enzymes typically lies in the range between 30 and 40 % when more strict NAC definitions are used [13].

3. Results and discussion

3.1. Protein characterization

CALB (wild type and Ser105Ala) was further purified by gel filtration [4] and freeze dried. An active-site titration with the inhibitor methyl *p*-nitrophenyl *n*-hexylphosphonate was performed on the freeze dried, non-immobilized enzyme [17]. This showed that 78% of the wild type enzyme was catalytically active. CD spectra (Jasco J-810) were recorded for wild type and Ser105Ala. The results showed that Ser105Ala had the same amount of correctly folded protein as the wild type enzyme. The mutant was therefore assumed to contain 78% active enzyme, based on the active-site titration of the wild type.

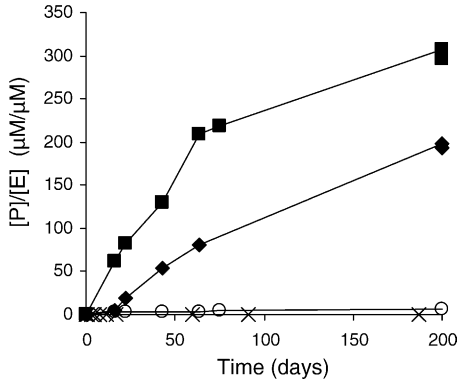

Fig. 1. Aldol reaction of hexanal catalyzed by CALB Ser105Ala, immobilized at pH 7.6 (♦) and 8.6 (■). The reaction catalyzed by imidazole (×) is as slow as the uncatalyzed reaction (◯). [P] is the total product concentration (aldol product and dehydrated product (α,β-unsaturated aldehyde)) and [E] is the enzyme concentration.

3.2. Aldol reaction

In our previous communication, we presented data showing that the reaction takes place in the active site (reactions were not catalyzed by covalently inhibited wild type enzyme, nor by albumin or empty carrier) [3]. We now present further evidence for the importance of the active site for efficient catalysis. Imidazole was tested as catalyst in an aldol reac-

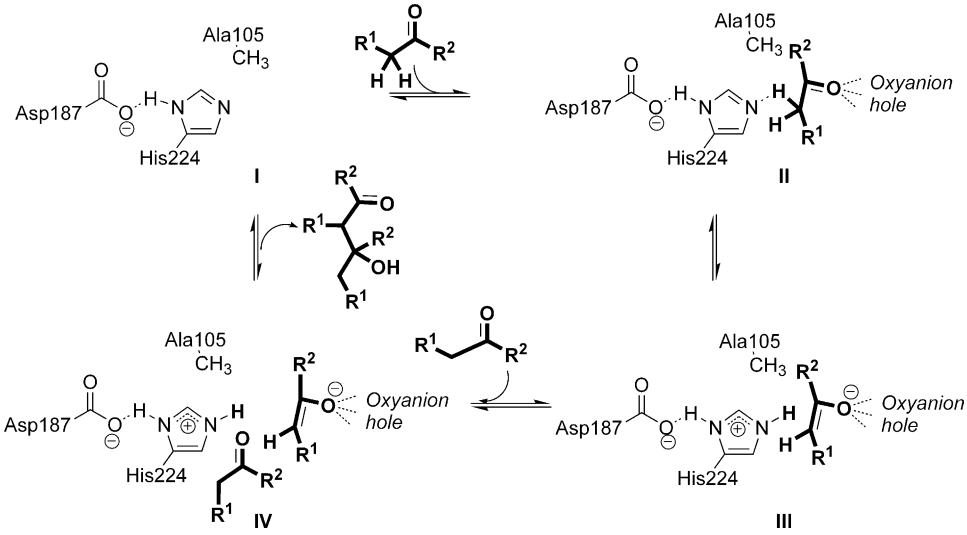

Scheme 2. Proposed reaction mechanism for aldol reaction in CALB Ser105Ala.

Table 1
The relative reaction rates compared to that of hexanal, **1**

Substrate[a]	Relative rate (substrate/hexanal)[b]
(**1**) R^1 = Bu, R^2 = H	1.0
(**2**) R^1 = Me, R^2 = H	0.65
(**3**) R^1 = *i*-Pr, R^2 = H	0.069
(**4**) R^1 = Bn, R^2 = H	0.053
(**5**) R^1 = Bn, R^2 = Me	0.027
(**6**) R^1 = H, R^2 = Me	0.013
(**7**) R^1 = Et, R^2 = Me	n.d.
(**8**) R^1 = Et, R^2 = Et	n.d.
(**9**) R^1 = Pr, R^2 = Et	n.d.

[a] For structure, see Scheme 1.
[b] Relative rate of total product formation (aldol and α,β-unsaturated product); n.d., product was not detected.

tion of hexanal in the absence of enzyme, without giving an increase in product formation compared to the uncatalyzed reaction (Fig. 1). The concentration of imidazole was similar to that of enzyme in other reactions. This shows that it is not solely the histidine that is responsible for the catalytic activity, but that the entire active site is needed.

In the reaction mechanism that we have suggested (Scheme 2) [3], the histidine needs to be in its unprotonated form in order to be active (abstracting the substrate's α-proton). This possible pH dependence was explored by immobilizing the enzyme either at pH 7.6 or 8.6. The enzyme immobilized at a higher pH was expected to show a higher activity. Enzymes show a "pH-memory", which means that it is possible to adjust the protonation state of an enzyme against a buffer with a specific pH and then still have this protonation state once the enzyme is dried [18]. Aldolization of hexanal was catalyzed with these two enzymes and the results showed a clear pH effect (Fig. 1). The enzyme that was immobilized at a higher pH showed a higher activity, supporting the proposed mechanism. During our experimental studies, it was also found that the reactions in water-saturated cyclohexane gave less of the unwanted dehydrated product, in favor of the aldol product. The concentration of the dehydrated product was decreased from about 10 to 15% of the total product concentration to only about 5%. Another lipase, *Pseudomonas cepacia* was also tested for activity for aldol reactions. This lipase also showed an activity in the same order as that of CALB WT, lower than the Ser105Ala mutant (data not shown). This shows that aldol reactions are also catalyzed by other serine hydrolases.

To explore the catalytic scope of CALB Ser105Ala, experiments were performed with a number of different aldehydes and ketones (Table 1). None of the tested substrates showed reaction rates over that of hexanal, although the enzyme showed activity towards substrates both with branched side-chains as well as phenyl groups. The lack of reactivity of **7**–**9** can be explained by their lower α-proton acidity. The pK_a values of the reacting substrates are below 16, whereas the non-reacting substrates show α-proton pK_a of around 19 [19].

As can be seen in Table 1, all aldol products formed, except for that from acetone, will have two stereocenters. This means that a total of four stereoisomeric products are possible and some stereodiscrimination can be expected. In the case of the aldol reaction of hexanal, we observed a change in diastereoselectivity, compared to the uncatalyzed reaction, but no or very low enantioselectivity. So far, we have not been able to come up with an explanation for this. One reason for the low enantioselection could be that the products are racemized.

3.3. Sequential reaction

In an attempt to find an explanation for the low reaction rate, equilibrium was also considered. A sequential reaction, in situ, was performed to displace the reaction from this eventual disfavored equilibrium position (Scheme 3, **a**). As mentioned earlier, one of the side products is the dehydrated product (α,β-unsaturated aldehyde/ketone) [20–22]. This is a substrate in a Michael-type addition, another reaction which has been shown to be catalyzed by CALB Ser105Ala [23]. By performing a sequential reaction, in situ, of an aldol addition (Scheme 3, **a**) followed by dehydration (Scheme 3, **b**) and finally a Michael-type addition (Scheme 3, **c**), it was expected that the final reaction step would cause a higher product formation in step **a**. This was however not seen and it could be concluded that the low reaction rate of the aldol addition was not due to an equilibrium problem. The first and third steps in this sequential reaction are catalyzed by CALB Ser105Ala.

3.4. Docking results

Since the reaction rates that were found experimentally were substantially lower than the theoretically predicted values (65 day^{-1} for hexanal), further studies were made in an attempt to find an explanation for this. Preliminary molecular dynamics data suggested that the distance between the substrate's α-proton and the histidine nitrogen (Nε2) was significantly longer than a normal hydrogen bond. This prompted us to explore the substrate binding more thoroughly. As the protein structure is not a static model, studies were made to verify if this long bonding distance was found in all cases or if a dynamic structure could position the active-site amino acids and the bound substrate at a closer distance.

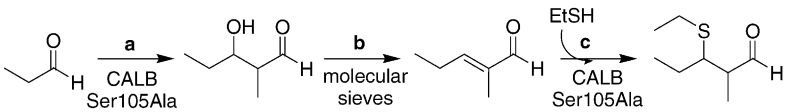

Scheme 3. A sequential, one-pot reaction of aldolization (**a**), dehydration (**b**) and a Michael-type addition (**c**).

The binding of the substrate hexanal was investigated using the automated docking procedure. The Autodock simulations showed that the first molecule of hexanal (Hex1) preferred to bind to the active site of the mutant, with a free energy of binding of −5.4 kcal/mol. The docked structure showed Hex1's carbonyl oxygen hydrogen bonded to the backbone amide hydrogens of amino acids Thr40 and Gln106, which are part of the oxyanion hole. The bond distances are 2.2 and 1.7 Å, respectively. Thr40's side-chain hydroxyl group can supply a third hydrogen bond to the oxyanion hole, but the hydroxyl group was turned away in the crystal structure and since the protein structure was kept static, no hydrogen bond between the substrate and Thr40's hydroxyl group was found. However, it was formed during MD simulations as discussed further. The first step of the mutant-catalyzed aldol addition has been predicted to be the enolization of Hex1 (Scheme 2, **II** → **III**), abstraction of the α-proton of Hex1 by His224. The distance, important for the catalysis of the reaction, between Nε2 of His224 and the α-carbon of Hex1 was found to be 4.2 Å in the docked structure. The free energy of binding for the second molecule of hexanal (Hex2) was −4.7 kcal/mol. All the docking runs found Hex2 in the active site of the mutant, where it seemed to bind through electrostatic interaction with amino acids Thr40, Trp104 and Leu278. The second step of the mutant-catalyzed aldol addition is the nucleophilic attack of the enol of Hex1 to the carbonyl carbon of Hex2 (Scheme 2, **IV** → product). The distance between the α-carbon of Hex1 and Hex2's carbonyl carbon was found to be 4.0 Å. Interestingly Hex2 was found to bind closer to His224 than Hex1 (3.0 Å compared to 4.2 Å). However, proton transfer between His224 and Hex2 instead of His224 and Hex1, as modeled in the previous communication [3], would be unlikely in the absence of any stabilizing hydrogen bonds between the enzyme and Hex2's carbonyl oxygen. In conclusion, the docking simulations predict both hexanals to bind to the active site. The two catalytically important distances, between Nε2 of His224 and the α-carbon of Hex1 and between the carbonyl carbon of Hex2 and the α-carbon of Hex1, are both longer than would be considered ideal for the reaction. However, the docking results only provide a static picture of the substrate binding and based on these results it cannot be ruled out that a high percentage of suitable near attack complexes are formed. Thus, the docking simulations are not sufficient to explain the very low reaction rate observed in experiments.

3.5. Molecular dynamics results

Selected protein–substrate complexes from the docking runs were used for subsequent MD simulations. The simulations were analyzed for the existence of near attack complexes (NACs). The first MD simulation has one molecule of hexanal bonded to the oxyanion hole of the mutant. During the entire simulation, the hexanal stays in the active site, for the most part forming at least two hydrogen bonds to the oxyanion hole. The strongest (shortest) hydrogen bond was found to be between the substrate and the side-chain hydroxyl group of Thr40. In our definition for the NAC of the proton transfer step of the aldol addition (enolization of the aldehyde/ketone, Scheme 2, **II**–**III**), the distance between Nε2 of His224 and the α-proton of hexanal should be in the proximity of the sum of their van der Waals radii (2.75 Å) [24] (Scheme 2, **II**). Analysis of this distance in the MD simulation showed that only 0.5% of the structures had a distance equal to or below this value. The mean distance between Nε2 of His224 and the closest α-proton of hexanal was 6.2 Å. When considering that the angle for proton transfer (Nε2–H–C) has not been taken into account for the definition of the NAC, it becomes clear that there is a very small amount of complexes that could lead to actual proton transfer.

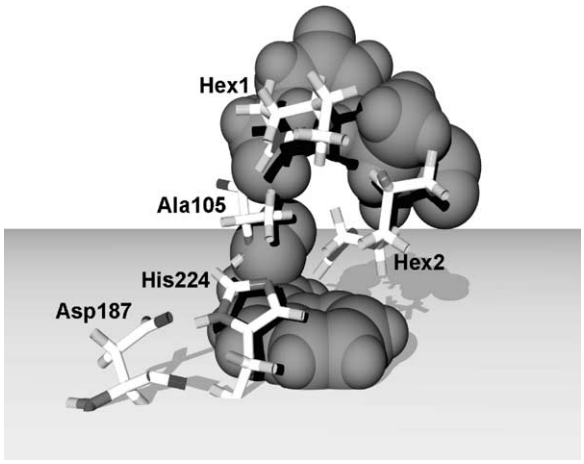

Fig. 2. Snapshot from the MD simulation of two hexanals (Hex1 and Hex2) bound to the active site of the Ser105Ala mutant of CALB, with an unprotonated His224. The amino acids forming the oxyanion hole (Gln106 and Thr40) and Trp104 are shown in spacefill.

Two MD simulations with two molecules of hexanal were performed. In the first simulation, His224 was unprotonated and the two substrate molecules were neutral. The dynamic simulation showed that the two molecules stayed in the active site during the entire simulation. In the second simulation, His224 was protonated and the hexanal, bound to the oxyanion hole was in its enolate form (Scheme 2, **IV**). All structures where the distance between the enolate's α-carbon and the carbonyl carbon of hexanal was less than the sum of the two atoms van der Waals radii (3.4 Å) [24] were considered to be NACs (see Fig. 2 for a snapshot of this simulation). A total of 2.2% of the structures were found to be NACs, with a mean distance of 4.8 Å. The low frequency of NACs together with the loose definition of the NAC indicates that also the second step of the aldol addition is slow.

In conclusion, the MD simulations show a low frequency of NACs for both the proton transfer step and the addition step of the aldol addition. The previous DFT calculations predicted an activation energy of 11.2 kcal/mol for the proton transfer and 15.1 kcal/mol for the addition step (both values are for acetaldehyde and relative the reactant complex). The activation energies are of the same magnitude as for natu-

ral enzymes. However, the low frequencies of NAC formation in the two steps will together lead to a large increase in the overall free energy of activation. Despite the rather loose NAC definitions employed in this work, the decrease in reaction rate can be estimated to be as large as three orders of magnitude, by multiplying the two NAC formation frequencies (0.5 and 2.2%). This effect together with the uncertainty in the computed activation barriers provides an explanation for the much lower reaction rate in the mutant compared to natural enzymes.

4. Conclusions

The experimental data presented show the importance of the entire active site for the lipase-catalyzed aldol addition of various substrates with the mutant Ser105Ala of *C. antarctica* lipase B. Furthermore, the slow rate of product formation was not caused by an unfavorable equilibrium position. This was explored by using a sequential reaction of an aldol addition followed by a Michael-type addition.

The low reaction rates of the aldol reaction in the lipase mutant was analyzed by molecular dynamic simulations, and was found to be caused by low frequencies of near attack complexes in the enzyme.

Acknowledgements

Financial support from the Swedish Research Council (VR) and from the Swedish Agency for Innovation Systems (VINNOVA) and computing resources from the Swedish National Allocations Committee (SNAC) is gratefully acknowledged.

References

[1] M. Holmquist, Curr. Protein Pept. Sci. 1 (2000) 209.
[2] J. Uppenberg, N. Öhrner, M. Norin, K. Hult, G.J. Kleywegt, S. Patkar, V. Waagem, T. Anthonsen, T.A. Jones, Biochemistry 34 (1995) 16838.
[3] C. Branneby, P. Carlqvist, A. Magnusson, K. Hult, T. Brinck, P. Berglund, J. Am. Chem. Soc. 125 (2003) 874.
[4] J.C. Rotticci-Mulder, M. Gustavsson, M. Holmquist, K. Hult, M. Martinelle, Protein Expr. Purif. 21 (2001) 386.
[5] L. Greenspan, J. Res. Nat. Bur. St. Phys. Chem. 81A (1977) 89.
[6] P. Ausloss, C.L. Clifton, S.G. Lias, A.I. Mikaya, S.E. Stein, D.V. Tchekhovskoi, O.D. Sparkman, V. Zaikin, D. Zhu, J. Am. Soc. Mass Spectrom. 10 (1999) 287.
[7] G.M. Morris, D.S. Goodsell, R.S. Halliday, R. Huey, W.E. Hart, R.K. Belew, A.J. Olson, J. Comput. Chem. 19 (1998) 1639 (See also www.scripps.edu/pub/olson-web/doc/autodock/).
[8] N. Guex, M.C. Peitsch, Electrophoresis 18 (1997) 27714 (See also http://www.expasy.org/spdbv/).
[9] S.J. Weiner, P.A. Kollman, D.A. Case, U.C. Singh, C. Ghio, G. Alagona, S.J. Profeta, P. Weiner, J. Am. Chem. Soc. 106 (1984) 765.
[10] B.H. Besler, K.M. Merz, P.A. Kollman, J. Comput. Chem. 11 (1990) 431.
[11] F.C. Lightstone, T.C. Bruice, J. Am. Chem. Soc. 118 (1996) 2595.
[12] F.C. Lightstone, T.C. Bruice, Acc. Chem. Res. 32 (1999) 127.
[13] S. Hur, T.C. Bruice, J. Am. Chem. Soc. 125 (2003) 1472.
[14] J. Marelius, K. Kolmodin, I. Feierberg, J. Åqvist, J. Mol. Graphics Modell. 16 (1998) 213.
[15] W.D. Cornell, P. Vieplak, C.I. Bayly, I.R. Gould, K.M. Merz, D.M. Ferguson, D.C. Spellmeyer, T. Fox, J.W. Caldwell, P.A. Kollman, J. Am. Chem. Soc. 117 (1995) 5179.
[16] W. Humphrey, A. Dalke, K. Schulten, J. Mol. Graphics Modell. 14 (1996) 33.
[17] D. Rotticci, T. Norin, K. Hult, M. Martinelle, Biochim. Biophys. Acta 1483 (2000) 132.
[18] E. Zacharis, P.J. Halling, D.G. Rees, Proc. Natl. Acad. Sci. U.S.A. 96 (1999) 1201.
[19] S.H. Hilal, S.W. Karickhoff, L.A. Carreira, Prediction of chemical reactivity parameters and physical properties of organic compounds from molecular structure using SPARC, US EPA Report EPA/600/R-03/030, March 2003 (Program available at: http://ibmlc2.chem.uga.edu/sparc).
[20] T. Hoffmann, G. Zhong, B. List, D. Shabat, J. Anderson, S. Gramatikova, R.A. Lerner, C.F. Barbas III, J. Am. Chem. Soc. 120 (1998) 2768.
[21] B. List, D. Shabat, G. Zhong, J.M. Turner, A. Li, T. Bui, J. Andersson, R.A. Lerner, C.F. Barbas III, J. Am. Chem. Soc. 121 (1999) 7283.
[22] B. List, R.A. Lerner, C.F. Barbas III, J. Am. Chem. Soc. 122 (2000) 2395.
[23] P. Carlqvist, M. Svedendahl, C. Branneby, K. Hult, T. Brinck, P. Berglund, ChemBioChem., in press.
[24] A. Bondi, J. Phys. Chem. 68 (1964) 441.